THE ASTROPHYSICAL JOURNAL, 524:849–856, 1999 October 10

THE DISCOVERY OF TWO NEW BIPOLAR PROTO–PLANETARY NEBULAE: IRAS 16594−4656 AND IRAS 17245−3951[1]

BRUCE J. HRIVNAK[2,3,4]
Department of Physics and Astronomy, Valparaiso University, Valparaiso, IN 46383; bruce.hrivnak@valpo.edu
AND
SUN KWOK[2,3,4] AND KATE Y. L. SU
Department of Physics and Astronomy, University of Calgary, Calgary T2N 1N4, Canada; kwok@iras.ucalgary.ca
Received 1998 September 22; accepted 1999 May 30

ABSTRACT

We report the discovery of two new, bipolar proto–planetary nebulae (PPNs). Both are cool *IRAS* sources for which we have confirmed optical counterparts by our 10 μm observations. Ground-based visible and infrared photometry was combined with the *IRAS* photometry and spectroscopy to produce their spectral energy distributions (SEDs). These SEDs look like those of other PPNs, in particular those of bipolar PPNs. The central stars of both objects are highly reddened and have color temperatures $\sim$3000–4000 K. The nebulosities are dominated by scattered light, not emission lines as in planetary nebulae. IRAS 16594−4656 appears to possess the 21 μm emission feature seen previously in a dozen carbon-rich PPNs, along with the 8 μm polycyclic aromatic hydrocarbon feature. Published millimeter-wave observations support the notion that it is carbon-rich, while IRAS 17245−3951 appears to be oxygen-rich. These facts confirm that these two objects are PPNs in transition between the asymptotic giant branch and planetary nebula phases. *Hubble Space Telescope* imaging reveals that they are indeed bipolar nebulae. IRAS 17245−3951 clearly displays two lobes separated by a dust lane; thus it is viewed nearly edge-on. Two jetlike features are seen in the southern lobe of IRAS 17245−3951, similar to the base of the searchlight beams seen in AFGL 2688. IRAS 16594−4656 appears to be a bipolar nebulae viewed at an intermediate orientation, and both the lobes and the central star can be seen. IRAS 16594−4656 therefore gives us our first clear example of the apparent morphology of a bipolar PPN viewed at an intermediate orientation. The addition of these objects to the list of bipolar PPNs confirms that such bipolar morphologies develop early in post-AGB evolution.

Subject heading: circumstellar matter — planetary nebulae: general — stars: AGB and post-AGB

1. INTRODUCTION

Planetary nebula (PN) represents an evolutionary phase that is passed through by most low- and intermediate-mass stars. Although over 1500 PNs have been cataloged, and over 10 times this number are believed to exist in the Galaxy, the immediate progenitors of PNs, commonly referred to as proto–planetary nebulae (PPNs), were, with a couple of exceptions, only discovered and studied in the last dozen years. PNs show strong emission-line spectra and are easy to identify by their spectra or morphologies. On the other hand, PPNs are difficult to find because their nebulosity is not ionized and can only be seen in scattered light. As a result, almost all the PPNs discovered to date have been first identified by their infrared characteristics; they all show a strong infrared excess due to circumstellar dust emission and have mid-infrared colors in between those of evolved asymptotic giant branch (AGB) stars and young PNs (Kwok 1993).

The most famous PPN is AFGL 2688 (the Egg Nebula), which shows bipolar lobes shining by scattered light from the F5 I central star (Latter et al. 1993). It was first found in the program of ground-based identification of Air Force Geophysics Laboratory (AFGL) sources by Ney et al. (1975). Similar bipolar PPNs have been found from ground-based identification of *IRAS* sources (e.g., IRAS 17150−3224 and IRAS 17441−2411; Kwok et al. 1996). The butterfly-like appearances of these objects are due to their orientations in the sky; they are nearly edge-on systems in which a dust torus conveniently obscures the bright central star, therefore allowing their bipolar lobes to be observed.

These recent discoveries suggest that nebulosities from other PPNs can be detected if their orientations are favorable. Ground-based imaging of PPNs has revealed a number of candidates with extended (nonstellar) structures (Hrivnak et al. 1999). The *Hubble Space Telescope* (*HST*), with its superior resolving power after the first service mission, has the potential to resolve the nebulosities from smaller or more distant PPNs. Spectacular, detailed images have been obtained with the *HST* of the bipolar nebulae AFGL 2688 (the Egg Nebula; Sahai et al. 1998a, 1998b), IRAS 17150−3224 (the Cotton Candy Nebula; Kwok, Su, & Hrivnak 1998), and IRAS 17441−2411 (the Silkworm Nebula, Su et al. 1998).

In this paper we report on the identification of the optical counterparts of two infrared-bright PPNs, IRAS 16594−4656 and 17245−3951. These two objects were first identified as PPNs by Volk & Kwok (1989) on the basis of

[1] This work was based on observations with the NASA/ESA Hubble Space Telescope, obtained at the Space Telescope Institute, which is operated by AURA, Inc., under NASA contract NAS5-26555.

[2] Visiting astronomer, United Kingdom Infrared Telescope, which is operated by the Royal Observatories on behalf of the UK Particle Physics and Astronomy Research Council.

[3] Visiting astronomer, Cerro Tololo Inter-American Observatory, National Optical Astronomy Observatories, which is operated by the Association of Universities for Research in Astronomy, Inc., under contract with the National Science Foundation.

[4] Visiting astronomer, Canada-France-Hawaii Telescope, which is operated by the National Research Council of Canada, the Centre National de Recherche Scientifique of France, and the University of Hawaii.

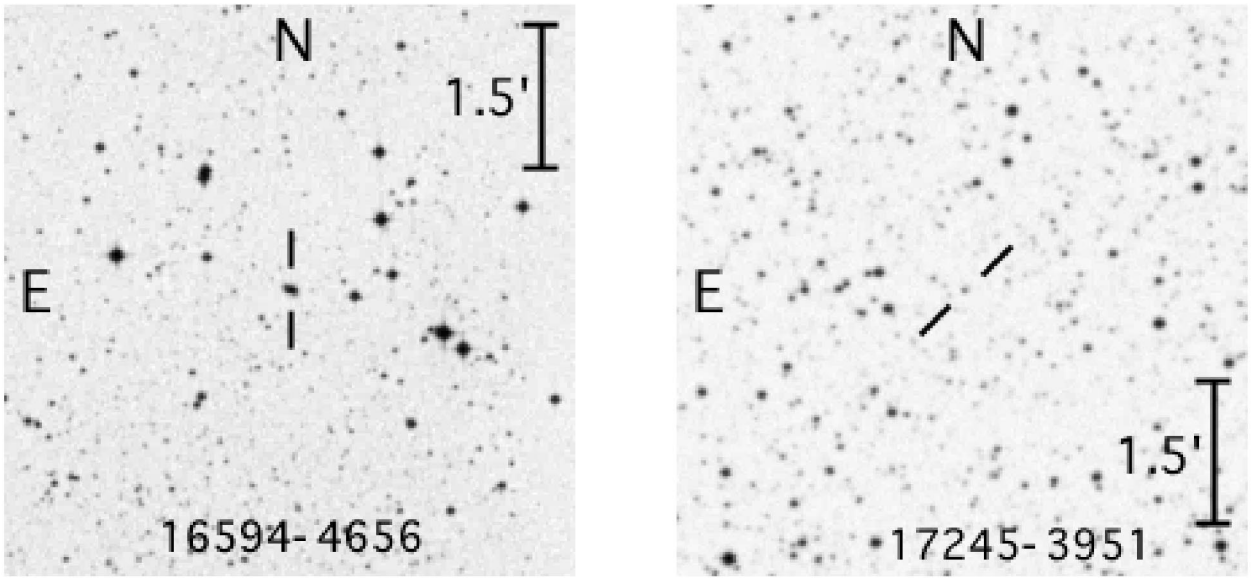

FIG. 1.—Finding charts of IRAS 16594−4656 and IRAS 17245− 3951, derived from the STScI Digital Sky Survey

their *IRAS* colors. We found likely optical counterparts, which we confirmed by ground-based mid-infrared observations; visible and infrared photometric measurements were made to define the spectral energy distribution (SED); and imaging revealed the objects to be extended. We then obtained visible images with the *HST*, which showed both objects to possess bipolar nebulae. These observations are discussed in this paper.

2. GROUND-BASED OBSERVATIONS

2.1. *Identification of Optical Counterparts*

An optical counterpart for IRAS 16594−4656 was suggested by transposing the *IRAS* position onto the Palomar Observatory Sky Survey print and noting a close positional association with a moderately bright object. The optical association was confirmed by observing strong mid-infrared flux from the star, using a bolometer on the 1.5 m telescope at Cerro Tololo Inter-American Observatory (CTIO) in 1992 May.

An optical counterpart for IRAS 17245−3951 was found by searching the area around the *IRAS* coordinates, using a bolometer at 10 μm. This was carried out on the 3.8 m United Kingdom Infrared Telescope (UKIRT) in 1989 August. We found the infrared source to be coincident with a moderately bright starlike object.

The finding charts of these two objects are given in Figure 1. Their coordinates, taken from the STScI Digitized Sky Survey, are listed in Table 1, along with their *IRAS* fluxes from the Faint Source Survey. IRAS 16594−4656 has an *IRAS* variability index of var = 34, which suggests a low possibility of variability, while IRAS 17245−3951 has var = 0, which indicates no evidence for variability.

2.2. *Visible and Infrared Photometry and Spectroscopy*

Follow-up ground-based visible and infrared photometry were carried out for both objects. The standardized photometric values are listed in Table 2. Both objects are quite red: $(B-V) = 1.71$ and $(V-I_c) = 2.60$ for IRAS 16594−4656 and $(V-I_c) = 2.34$ for IRAS 17245−3951. Visible CCD imaging revealed both objects to be extended. The imaging of IRAS 17245−3951, carried out at the Canada-France-Hawaii Telescope (CFHT), is discussed elsewhere as part of our survey of the shapes of resolved PPNs (Hrivnak et al. 1999).

A visible spectrum of IRAS 16594−4656 was obtained on 1992 May 13 with the 2D-Frutti spectrograph on the 1.0 m Yale telescope at CTIO. The system uses a photon-counting detector, and a spectrum was acquired over the range 3700–7200 Å at a resolution of 7.5 Å. Two 40 minute spectra were obtained and combined. The object is relatively faint for the system, especially in the blue, and the resulting signal-to-noise ratio of the spectrum is low. It possesses an Hα emission feature, with an equivalent width of 28.3 Å and possibly weak emission at Hβ. The rest of the spectrum appears featureless, with a continuum shape like that of a very cool star, although much of that is presumably due to reddening. Note that W. P. Bidelman (1989, private communication) called attention to the likely association of IRAS 16594−4656 with object 293 in the catalog of

TABLE 1

POSITIONS AND *IRAS* FLUXES

IRAS Identification	R.A. (J2000)	Decl. (J2000)	l (deg)	b (deg)	F_{12} (Jy)	F_{25} (Jy)	F_{60} (Jy)	F_{100} (Jy)
16594−4656.....	17 03 10.0	−47 00 27	340.4	−3.3	45	288	118	30:
17245−3951.....	17 28 04.6	−39 53 44	348.8	−2.8	2.7	44	34	<13

NOTE.—Units of right ascension are hours, minutes, and seconds, and units of declination are degrees, arcminutes, and arcseconds.

TABLE 2

GROUND-BASED VISIBLE AND INFRARED PHOTOMETRY

IRAS Identification	B	V	R_c[a]	I_c[a]			Observatory	Date
16594−4656.....	16.31 ± 0.03	14.60 ± 0.02	13.27 ± 0.03	12.00 ± 0.04			CTIO	1992 May 19
17245−3951.....	...	15.50 ± 0.01	...	13.16 ± 0.02			CFHT	1991 Jun 05
	J	H	K	L	L'	M'		
17245−3951.....	11.34	10.40	9.71	...	...	...	SAAO[b]	1988 Mar 02
	11.33	10.39	9.70	8.93 ± 0.09	...	...	SAAO[b]	1988 Mar 31
	11.38 ± 0.05	10.54 ± 0.05	9.85	...	8.91	8.14 ± 0.09	UKIRT	1989 Aug 17
	8.75 μm	9.7 μm	N	11.5 μm	12.5 μm	Q		
17245−3951.....	4.88 ± 0.19	4.08 ± 0.20	3.59 ± 0.11	2.61 ± 0.05	2.36 ± 0.07	− 0.91 ± 0.04	UKIRT	1990 Aug 22

NOTE.—The uncertainty in the near-infrared photometry is less than ±0.05, unless otherwise indicated.

[a] The R and I magnitudes are in the Cousins system.

[b] Near-infrared photometry was kindly carried out by P. Whitelock at the South African Astronomical Observatory (SAAO).

Hα emission stars by Stephenson & Sanduleak (1977). In this catalog it is classified as Hα (weak) with $m_V = 13.5 \pm 1.0$. This appears to be the same star that we have confirmed as the optical counterpart.

3. *HST* WFPC2 IMAGING

Using the Wide-Field Planetary Camera 2 (WFPC2) of the *HST*, we have imaged IRAS 16594−4656 and 17245−3951. We used the planetary camera and the wide-band filter F606W ($\langle\lambda\rangle = 584$ nm, $\Delta\lambda = 158$ nm). The data were obtained in 1997 March as part of program 6565 (PI: S. Kwok). A total of nine exposures were taken for each object, with integration times of 4 × 20 s, 4 × 120 s, and 1 × 260 s for IRAS 16594−4656, and 4 × 20 s, 4 × 120 s, and 1 × 200 s for IRAS 17245−3951. In the longer exposures of IRAS 16594−4656, the image of the central star is saturated. Standard bias and dark subtraction and flat-field corrections were performed. We took our data in a four-point dithered pattern to permit an improvement in the combined image resolution. Since the WFPC2 undersamples the image, the technique of linear recombination of images, called "drizzling" (Fruchter & Hook 1997), was used to reconstruct the point-spread function (PSF). The PSF after drizzling is found to have a FWHM of 0.″07.

Figure 2*a* shows the image of IRAS 17245−3951 derived from the combined 480 s drizzled image. The image has also been deconvolved with the theoretical PSF, using the "maximum entropy method." This led to a slight improvement in the contrast of the features, but all of the features seen in the deconvolved image are seen in the original image. A bipolar structure is clearly seen, with a well-defined dark obscuring lane between the two lobes. The lobes are approximately equal in size, but the northern lobe is brighter, with a flux ratio of 1.63. The total size of the lobes is 2.″23 × 0.″6, where we have measured the size of the lobes by the level at which the flux is 1% of the peak value.

If we assume that the two lobes have the same intrinsic brightness, then the fact that the north lobe is brighter than the south lobe suggests that it is tilted toward us, with the south lobe suffering from extinction. If this is the case, it would suggest that the obscuring region is large in size, on the order of the size of the lobes. The orientation of the nebula is ∼11°, measured from north to east, as determined from the brightness peak in each lobe. As measured from the outer brightness contours of the nebula, the orientation is ∼1°. Assuming that the direction of the major axis represents the direction of a collimated outflow, the difference of 10° could be attributed to a change in the orientation of the collimating region.

The image of IRAS 17245−3951 also shows some structure in the lobes, especially the south lobe, in which we see what appears to be a second brightness peak and also two approximately parallel "jetlike" features pointing away from the obscuring region. These features resemble the spindle-shaped features at the base of the beams seen in the southern lobe of the Egg Nebula (Sahai et al. 1998a, their Fig. 1*c*). We believe that these features are not physical ejecta but rather represent reflections from the walls of a central cavity. The lobes are surrounded by an extended faint halo of size 2.″8 × 2.″1, as measured where the flux density contour is at a level of 10 $\sigma_{\rm sky}$ level above sky background (where $\sigma_{\rm sky}$ is the uncertainty in the sky level). This halo is brought out more clearly in our false-color image in Figure 2*b*. Based on the general appearance of the nebula, we have named IRAS 17245−3951 the "Walnut Nebula."

Figures 3*a* and 3*b* show images of IRAS 16594−4656 derived from the 80 and 480 s drizzled images. Again the images have been sharpened slightly by deconvolution. In the shorter exposure, we can clearly see the image of the central star, which has a position of R.A.(2000.0) = $17^{\rm h}03^{\rm m}10^{\rm s}.00$ and decl.(2000.0) = −47°00′26.″9. In the longer exposure, which we display in false color, the central star is saturated, and we can see more of the complex outer structure. The size of the brighter central part of the nebula is 4.″6 × 2.″2, where we have measured this at the level at which the flux density is 10 $\sigma_{\rm sky}$ above sky. If we measure the contour at the 3 $\sigma_{\rm sky}$ level above sky, the size is 6.″3 × 3.″3. The star directly contributes ∼25% of the total light of the object through this filter.

The morphology of the nebula resembles that of a flower, and we name it the "Water Lily Nebula." The outer "petals" of the nebula extend to 6.″4 from the star. The position of the central star within the nebula suggests that one is seeing a bipolar nebula at some intermediate viewing angle rather than nearly edge-on, as is apparently the case for IRAS 17245−3951.

The outer petals appear to point approximately outward from the central star. In fact, one can identify three main petals on opposite sides of the nebula that appear to be nearly symmetrical about the central star. These are identi-

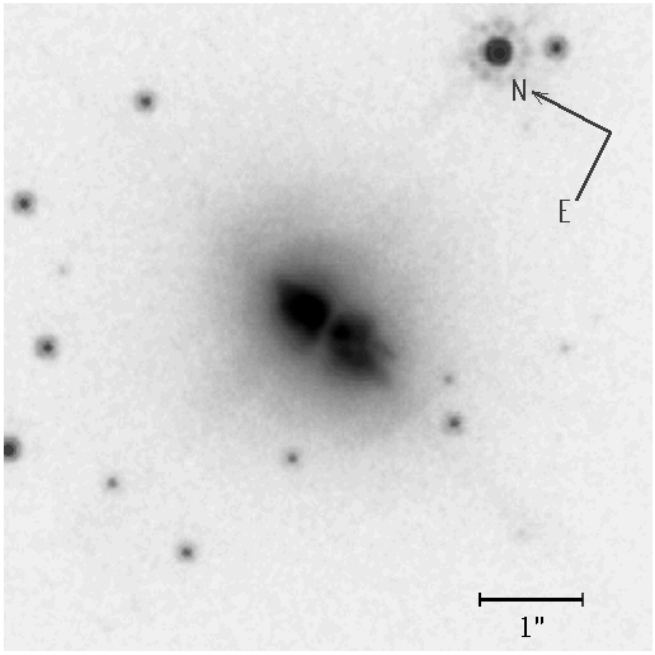

FIG. 2*a*

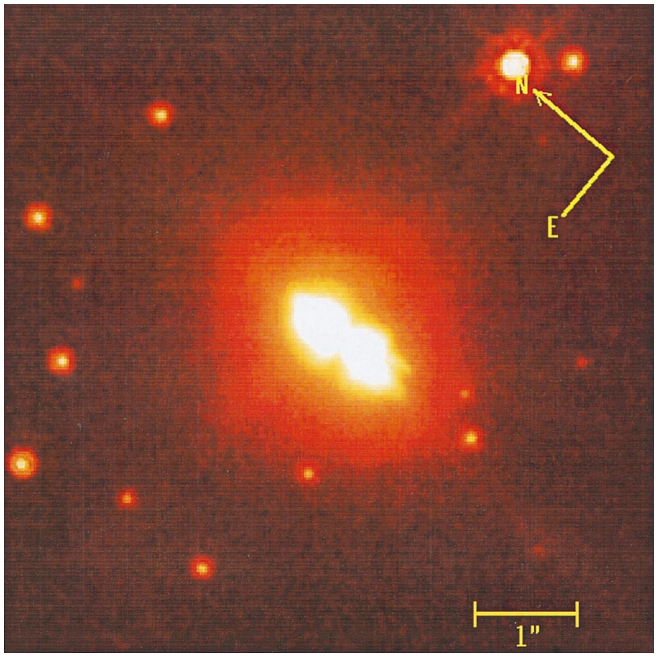

FIG. 2*b*

FIG. 2.—*HST* WFPC2 F606W image of IRAS 17245−3951, with the long exposure (480 s total): (*a*) Gray-scale image showing the brighter regions of the nebula and the dark obscuring lane between the lobes. (*b*) False-color image, emphasizing the fainter halo.

fied in Figure 4*a*. The petals extending toward the southwest are slightly longer than the oppositely directed ones. The length on both sides decrease in the counterclockwise direction. There appears to be an "S"-shaped pattern to the shorter and brighter two pairs of petals, suggesting rotation in the counterclockwise direction. This is the same direction in which the lengths appear to decrease. This suggests oppositely directed material ejected episodically from a rotating source. Similar structures are also seen in PNs (e.g., Fig. 1, López, Roth, & Tapia 1993; KjPn 8, López, Vázquez, & Rodriguez 1995; Sahai & Trauger 1998). If these point-symmetric structures are indeed related, then it suggests that they originate during the PPN phase before photoionization.

The "flower-like" morphology of IRAS 16594−4656 bears some similarity with the bipolar PN NGC 6302 (shown for comparison in Fig. 4*b*). It appears that IRAS 16594−4656 may have a similar hourglass structure, with

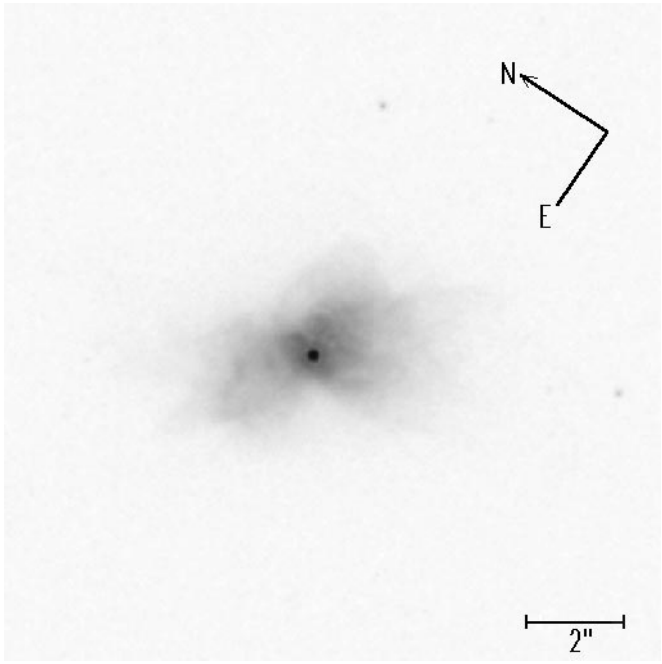

FIG. 3*a*

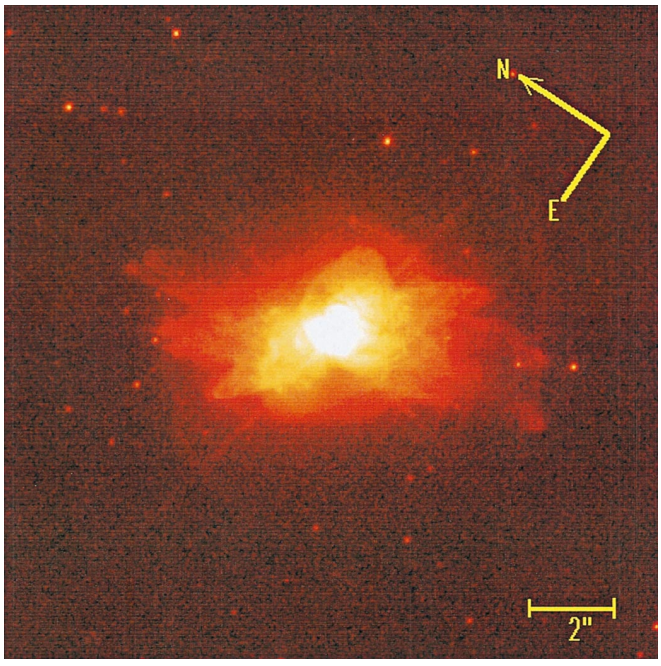

FIG. 3*b*

FIG. 3.—*HST* WFPC2 F606W images of IRAS 16594−4656: (*a*) Gray-scale image with the short exposure (80 s total), which shows the central star clearly. (*b*) False color-image with the long exposure (480 s total), which shows the fainter outer structure.

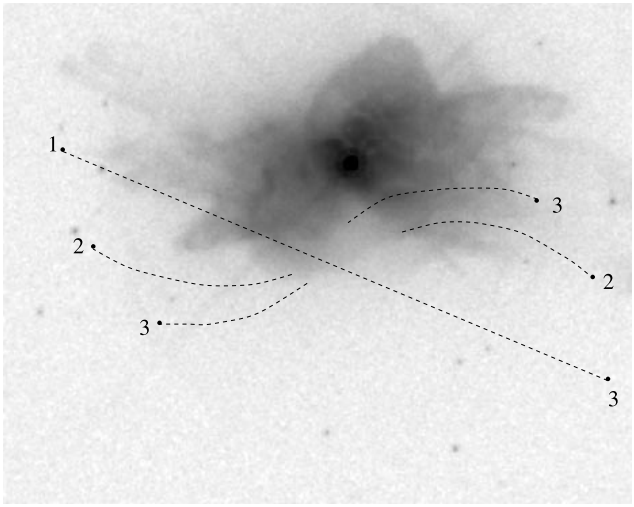

FIG. 4*a*

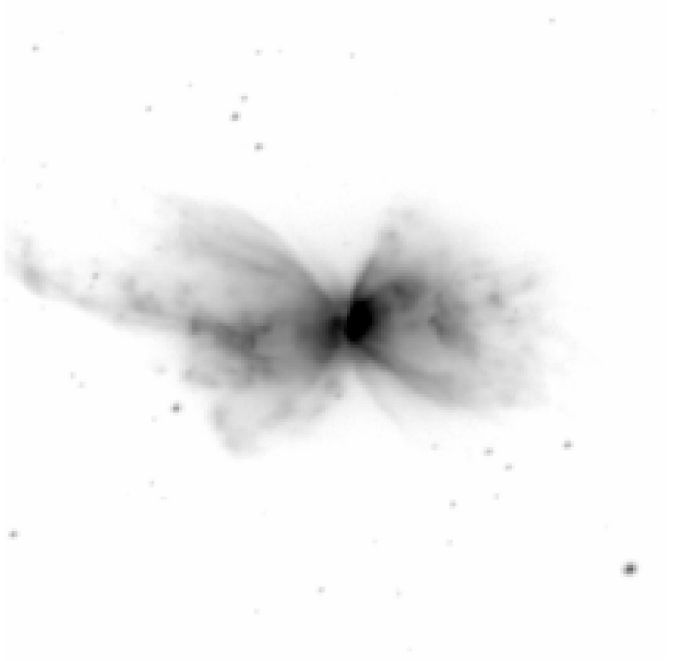

FIG. 4*b*

FIG. 4.—(*a*) *HST* image of IRAS 16594−4656 with some of the suggested structure outlined. (*b*) Hα image of NGC 6302 (north is to the left, and east is up; Hua, Dopita, & Martinis 1998) for comparison.

the petals extending out from this basic structure. As IRAS 16594−4656 evolves into a PN, it will probably develop a similar ionization-bounded equatorial region, and NGC 6302 could just represent a more evolved, more edge-on version of IRAS 16594−4656.

4. DISCUSSION

4.1. *The SEDs*

The SEDs for these two sources can be formed from 0.5 to 100 μm, based on our new photometry together with the *IRAS* photometry and spectroscopy. For IRAS 16594−4656, we have also included observations by van der Veen, Habing, & Geballe (1989), who published infrared photometry but who apparently did not note the existence of the optical counterpart. Similar near-infrared values for IRAS 16594−4656 were recently published by García-Lario et al. (1997). Since both objects lie at low Galactic latitudes, interstellar extinction is expected to significantly affect the flux at shorter wavelengths. We estimate $A_v \simeq 3.2$ mag for IRAS 16594−4656 (for a distance of >1.3 kpc) and $A_v \simeq 1.6$ mag for IRAS 17245−3951 (Neckel & Klare 1980). We have thus corrected the observed fluxes for extinction using these estimated values and the interstellar extinction law of Cardelli, Clayton, & Mathis (1989). The extinction-corrected SEDs are displayed in Figure 5. The SED for IRAS 16594−4656 is dominated by a strong mid-infrared peak due to dust emission ($T_d \sim 160$ K) with a plateau leading to a smaller peak in the near-infrared, and it drops down again in the visible. This is similar to the shape of the SEDs seen in the bipolar PPNe such as AFGL 2688, IRAS 17441−2411, and IRAS 17150−3224 (Hrivnak & Kwok 1991; Kwok et al. 1996). The total flux in the dust component of IRAS 16594−4656 is $\sim 5 \times 10^{-8}$ ergs cm^{-2} s^{-1}, and the total flux in the photospheric component is about 30 times smaller ($\sim 1.5 \times 10^{-9}$ ergs cm^{-2} s^{-1}). These observed fluxes give a minimum luminosity of ~ 1600 $(D/\text{kpc})^2$ $L_\odot$. The SED for IRAS 17245−3951 is similarly dominated by a strong mid-infrared peak due to emission from dust ($T_d \sim 140$ K; total flux $\sim 7 \times 10^{-9}$ ergs cm^{-2} s^{-1}). The flux ratio between the dust-to-photospheric components (~ 30) is similar to that observed in IRAS 16594−4656. Since this is a bipolar nebula viewed near edge-on, some of the stellar flux will be escaping in the polar directions, and the actual total flux emitted by the object will be higher. Ignoring the missing stellar flux in the polar directions, the total flux for IRAS 17245−3951 is 7×10^{-9} ergs cm^{-2} s^{-1}, or ~ 220 $(D/\text{kpc})^2$ $L_\odot$. Note that before the extinction correction, the photospheric temperatures of IRAS 16594−4656 and 17245−3951 appeared to be much lower, 2200 and 2500 K, respectively, and the dust-to-photospheric flux ratios appeared to be much higher, ~ 100 and ~ 40, respectively.

Mid-infrared spectra of both sources were obtained with the Low Resolution Spectrometer (LRS) aboard *IRAS*. A good spectrum of the bright source IRAS 16594−4656 was obtained; the spectrum was classified as type = 74 in the Atlas of Low-Resolution *IRAS* Spectra (1986), which indicates a 10 μm silicate absorption feature on a red continuum. It was subsequently recalibrated following the procedures of Volk & Cohen (1989) and classified as type = *P*, which indicates the presence of polycyclic aromatic hydrocarbons (PAH) features in emission, rather than an absorption feature at 10 μm (Kwok, Volk, & Bidelman 1997). It shows a strong emission feature at 8 μm, which can be attributed to PAHs, and an emission feature at 21 μm. The LRS spectrum of IRAS 17245−3951 is much weaker and is basically noise at the shorter wavelength band, and it rises steeply at longer wavelengths. The shapes of these mid-infrared spectra can be seen in Figure 5. (Note that we have not plotted the short wavelength band for IRAS 17245−3951.)

The detection of a likely 21 μm feature in IRAS 16594−4656 is quite interesting. Twelve such sources are

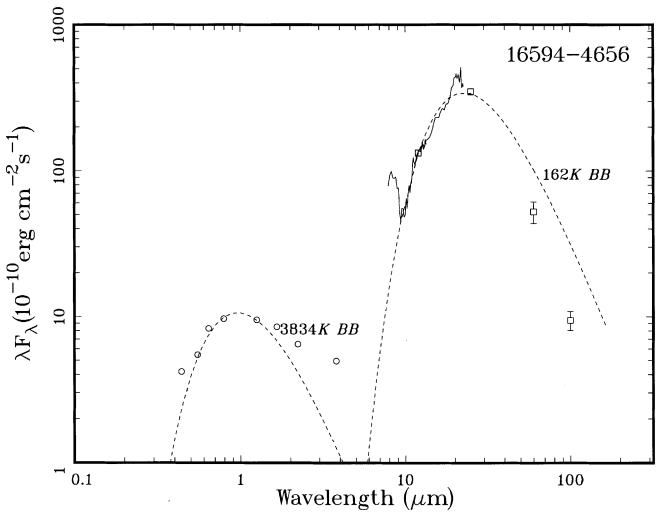

FIG. 5a

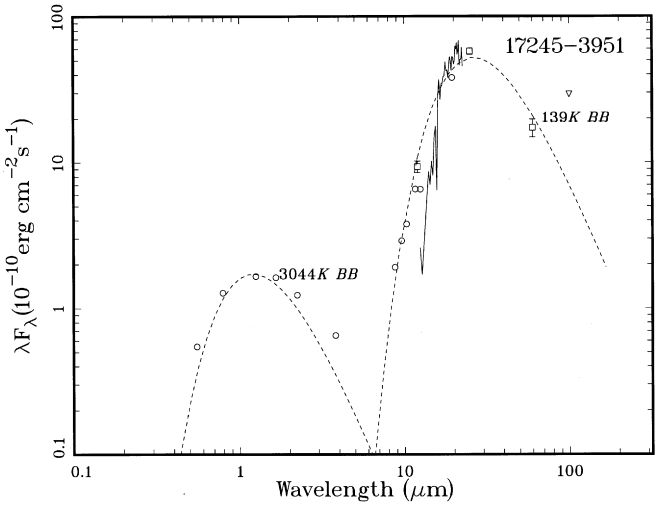

FIG. 5b

FIG. 5.—SEDs of IRAS 16594−4656 and IRAS 17245−3951. The circles and squares are ground-based and *IRAS* (color-corrected) photometric measurements, respectively. For IRAS 16594−4656, we have included near-infrared data from van der Veen et al. (1989). The visible and near-infrared fluxes have been corrected for interstellar extinction, as described in the text. Two blackbodies are fitted to the photospheric and dust components, with the color temperatures shown above each curve.

presently known, and all are carbon-rich PPNs with central stars displaying G or F supergiant spectra (Kwok, Volk, & Hrivnak 1999).

4.2. *The PPN Nature of These Sources*

The first clue that IRAS 16594−4656 and 17245−3951 are objects in the transition stage between the AGB and PN phases is provided by their SEDs. Objects in the preceding evolutionary stage, evolved AGB stars, have their dust envelopes attached to their photosphere and are often totally obscured by the dust envelope ($T_d \geq 300$ K). PNs, the succeeding stage, have much hotter central stars, and most of their photon output is reprocessed into nebular emission. Their SEDs show blackbody-like dust continua of lower temperatures ($T_d \sim 50$–150 K) due to the dispersing AGB dust envelope (Zhang & Kwok 1991). PPNs, with their central stars' photospheric emission peaking in the visual and near-infrared range and with lower circumstellar extinction than AGB stars due to the fact that the dust envelopes are detached from the photospheres, have unique, doubled-peaked SEDs ($T_d \sim 150$–300 K). Comparison of the SEDs of these two objects with other known PPNs (Kwok 1993) indicates that the SEDs of these two objects are consistent with the SEDs of PPNs.

While the appearance of IRAS 16594−4656 shows similarities to the young PN NGC 6302, the optical spectra are different. PNs are defined by their emission-line spectra because of recombination lines of H and He and forbidden lines of metals. A higher signal-to-noise ratio spectrum of this object is presented by García-Lario et al. (1999). In addition to the strong Hα emission, Hβ is clearly seen in emission along with [O I] emission at 6300 Å. The existence of Hα emission is not uncommon among PPNs (Hrivnak & Woodsworth 1993; Oudmaijer & Bakker 1994), and it may be due to ongoing low-level mass loss or to shocks related to pulsation in these objects (Lébre et al. 1996; Hrivnak & Lu 1999). Also, a search for 6 cm radio emission, expected from the ionized region and commonly seen among PNs, resulted in no detection for IRAS 16594−4656 (Van de Steene & Pottasch 1993).

Since young stellar objects (YSOs) and massive stars evolving to the blue from the red supergiant stage may also possess bipolar, detached circumstellar envelopes, the nebular properties alone are not sufficient to distinguish PPNs from these objects. CO (1–0) emission has been detected from IRAS 16594−4656, with an expansion velocity of $V_{\rm exp} \geq 16$ km s^{-1} (Loup et al. 1990), while OH (1612 MHz) maser emission has been detected from IRAS 17245−3951, with a typical double-peaked spectrum and with $V_{\rm exp} = 11.7$ km s^{-1} (Sevenster et al. 1997). The CO line widths observed in YSOs are often narrow, and supergiants have larger expansion velocities. The expansion velocities observed in these two objects are in the range of typical of wind expansion velocities (10-20 km s^{-1}) of AGB stars, suggesting that the molecular envelopes of these two objects are indeed remnants of AGB circumstellar envelopes.

The presence of the 21 μm feature in IRAS 16594−4656 is also consistent with its PPN nature. The 21 μm feature, confirmed by *ISO* spectroscopy by García-Lario et al. (1999), has never been detected in PNs, YSOs, or massive supergiants, and all the 21 μm sources known to date are PPNs (Kwok et al. 1999).

The chemistry of IRAS 16594−4656 appears to be carbon-rich. This is based in part upon the detection of CO but not OH (te Lintel Hekkert et al. 1991) and in part on the presence of unidentified IR emission features found at 3.3, 6.2, 7.7, 8.6, 11.3, 12.7, and 13.5 μm as well as the 21 μm feature (García-Lario et al. 1999). IRAS 17245−3951 appears to be oxygen-rich, based on the detection of OH maser emission from the source. Although a complete photospheric abundance analysis would give conclusive evidence of their PPN nature (Van Winckel 1999), high-resolution optical spectroscopy is not easy for these faint sources. However, their circumstellar chemistry is consistent with they being post-AGB stars.

4.3. *Bipolar Morphologies in PPNs*

One of the major unsolved questions in the study of PNs is how and when their morphologies develop. The discovery and imaging of PPNs plays an important role in finding answers to these questions (Kwok et al. 1996). The *HST* images reported in this paper confirm that bipolar or even

point-symmetric morphologies are common in PPNs. Clues to the geometry of the system can also be found in the SED observed. The dust emission from PPNs is generally optically thin and is independent of viewing angle, whereas the photospheric component, made up of directly attenuated starlight and dust-scattered starlight, is sensitive to viewing angle. At a small viewing angle ($i \sim 0°$, or near edge-on), the star is obscured by the equatorial dust, and only a small fraction of the stellar flux is observed. The dust-to-photospheric bolometric flux ratios observed in PPNs range from ~ 1 to $\sim 10^3$ (Hrivnak & Kwok 1991), and the two objects reported in this paper are in the middle of the range. For objects with approximately equal dust and photospheric flux components (e.g., IRAS 18095+2704; Hrivnak, Kwok, & Volk 1988), the orientations are probably nearly pole-on, and their nebulosities would be difficult to observe because of the strong direct starlight. It would therefore be difficult to obtain direct evidence of their bipolar nature, even though they may have similar intrinsic structures to observed bipolar nebulae.

We note that, based on the above general discussion of the relationship of the dust-to-photospheric flux ratios with viewing angle, we would have expected the ratio of IRAS 17245−3951 to be higher than that of IRAS 16594−4656. Instead, they are approximately the same. Other factors, such as the optical depth of the obscuring dust, also affect this ratio. In this case, we would expect the optical depth for IRAS 17245−3951 to be not as large as that of AFGL 2688, which is also an edge-on PPN, for which the dust-to-photospheric ratio is very high ($\sim 10^3$). This appears to be borne out observationally by the Near-Infrared Camera and Multiobject Spectrometer J-band detection of the central star of IRAS 17245−3951 (Kwok et al. 1998b) but not of AFGL 2688 (Sahai et al. 1998b). Thus, while the SED can give a general clue to the geometry of a system, high-resolution images are needed to reliably determine the morphology.

The *HST* image of IRAS 17245−3951 clearly shows two bipolar lobes separated by a dust lane. This suggests that the system is being viewed nearly edge-on. The fact that the central star can be seen in IRAS 16594−4656 and the nebulosity has a less obvious bipolar structure suggests that it is oriented at an intermediate angle. While the details of how the appearance of a bipolar PPN changes with viewing angle will depend upon the specific properties of the obscuring region, the morphology of IRAS 16594−4656 nevertheless provides us with a clear example of one such intermediate-angle PPN.

The addition of these objects to the list of bipolar PPNs confirms that such bipolar morphologies develop early in post-AGB evolution. These PPNs will provide the crucial link in our understanding of the origin of bipolar structures in PNs.

5. CONCLUSIONS

We have discovered two new PPNs from among low-temperature sources selected from the *IRAS* catalog. Both show double-peaked SEDs characteristic of PPNs, suggesting that the dust envelopes have detached from the photospheres and the large-scale mass-loss phase on the AGB has ended. The LRS spectrum of IRAS 16594−4656 shows the 21 μm emission feature which is seen in several other PPNs. The optical spectrum of IRAS 16594−4656 is consistent with a reddened photosphere and not a photoionized region, suggesting that these stars are still evolving toward the PN stage.

The discovery of these two objects reiterates the success of the identification of PPNs from cool *IRAS* sources. Over 30 objects have been identified in this way, with nearly homogeneous properties. While some *IRAS* PPN candidates are associated with bright, starlike objects, and others show nebulosities around faint central stars, we believe that they all have similar intrinsic structures. The optically bright sources are likely to be viewed along the polar directions, whereas the optically faint sources have their central stars obscured by equatorial dust. While the nebulosities of pole-on objects are difficult to observe because of the bright direct starlight, the surrounding nebulosity of edge-on objects can be seen in scattered light. The optical images of IRAS 17245−3951 and 16594−4656 presented in this paper provide illustrations of systems that are viewed at nearly edge-on and at intermediate orientations, respectively. These complementary images give us useful clues on the intrinsic three-dimensional structures of the still-neutral nebulae and will help us understand the mechanism of how PNs are shaped.

We acknowledge the assistance of P. Langill in part of the ground-based observing and B. E. Reddy with the reduction of the optical spectrum, and thank P. Whitelock for making near-infrared observations of one of these sources. Following our initial submission of this paper, P. García-Lario kindly sent us a preprint of his paper on IRAS 16594−4656, to which we have subsequently made reference. This research made use of the Simbad database, operated at CDS, Strasbourg, France. This work is supported in part by NASA grants to B. J. H. through NASA/JOVE (NAG 8-232) and through grant number GO-06565.01-95A from the Space Telescope Science Institute, which is operated by the Association of Universities for Research in Astronomy, Inc., under NASA contract NAG5-26555, and in part by a grant to S. K. from the Natural Science and Engineering Research Council of Canada.

REFERENCES

Atlas of Low Resolution *IRAS* Spectra. 1986, *IRAS* Science Team, prepared by F. M. Olnon & E. Raimond, A&AS, 65, 607
Cardelli, J. A., Clayton, G. C., & Mathis, J. S. 1989, ApJ, 345, 245
Fruchter, A. S., & Hook, R. N. 1997, Proc. SPIE, 3164, 120
García-Lario, P., Manchado, A., Pych, W., & Pottasch, S. R. 1997, A&AS, 126, 479
García-Lario, P., Manchado, A., Ulla, A., & Manteiga, M. 1999, ApJ, 513, 941
Hrivnak, B. J., & Kwok, S. 1991, ApJ, 368, 564
Hrivnak, B. J., Kwok, S., & Volk, K. M. 1988, ApJ, 331, 832
Hrivnak, B. J., Langill, P. P., Su, K. Y.-L., & Kwok, S. 1999, ApJ, 513, 421
Hrivnak, B. J., & Lu, W. 1999, in IAU Symp. 177, Carbon Stars, ed. R. Wing (Dordrecht: Kluwer), 293
Hrivnak, B. J., & Woodsworth, A. W. 1993, in IAU Symp. 155, Planetary Nebulae, ed. R. Weinberger & A. Acker (Dordrecht: Kluwer), 354
Hua, C. T., Dopita, M. A., & Martinis, J. 1998, A&AS, 133, 361
Kwok, S. 1993, ARA&A, 31, 63
Kwok, S., Hrivnak, B. J., Zhang, C. Y., & Langill, P. L. 1996, ApJ, 472, 287
Kwok, S., Su, K. Y.-L., & Hrivnak, B. J. 1998a, ApJ, 501, L117
Kwok, S., Su, K. Y. L., Hrivnak, B. J., Sahai, R., & Dayal, A. 1998b, BAAS, 193, 1273
Kwok, S., Volk, K., & Bidelman W. P. 1997, ApJS, 112, 557

Kwok, S., Volk, K., & Hrivnak, B. J. 1999, in IAU Symp. 191, Asymptotic Giant Branch Stars, ed. T. Le Bertre, A. Lébre, & C. Waelkens (San Francisco: ASP), 297
Latter, W. B., Hora, J. L., Kelly, D. M., Deutsch, L. K., & Maloney, P. R. 1993, AJ, 106, 260
Lébre, A., Mauron, N., Gillet, D., & Barthes, D. 1996, A&A, 310, 923
López, J. A., Roth, M., & Tapia, M. 1993, A&A, 267, 194
López, J. A., Vázquez, R., & Rodriguez, L. F. 1995, ApJ, 455, L63
Loup, C., Forveille, T., Lyman, L. A., & Omont, A. 1990, A&A, 227, L29
Neckel, T., & Klare, G. 1980, A&AS, 42, 251
Ney, E. P., Merrill, K. M., Becklin, E. E., Neugebauer, & G., Wynn-Williams, C. G. 1975, ApJ, 198, L129
Oudmaijer, R. D., & Bakker, E. J. 1994, MNRAS, 271, 615
Sahai, R., & Trauger, J. T. 1998, AJ, 116, 1357
Sahai, R., et al. 1998a, ApJ, 493, 301
Sahai, R., et al. 1998b, ApJ, 492, L163
Sevenster, M. N., Chapman, J. M., Habing, H. J., Killeen, N. E. B., & Lindqvist, M. 1997, A&AS, 124, 509
Stephenson, C. B. & Sanduleak N. 1977, ApJS, 33, 459
Su, K. Y.-L., Volk, K., Kwok, S., & Hrivnak, B. J. 1998, ApJ, 508, 744
te Lintel Hekkert, P., Caswell, J. L., Habing, H. J., Haynes, R. F., & Norris, R. P. 1991, A&AS, 90, 327
Van de Steene, G. C. M., & Pottasch, S. R. 1993, A&A, 274, 895
van der Veen, W. E. C. J., Habing, H. J., & Geballe, T. R. 1989, A&A, 226, 108
van Winckel, H. 1999, in IAU Symp. 191, Asymptotic Giant Branch Stars, ed. T. Le Bertre, A. Lébre, & C. Waelkens (San Francisco: ASP), 465
Volk, K., & Cohen M. 1989, AJ, 98, 931
Volk, K. M., & Kwok, S. 1989, ApJ, 342, 345
Zhang, C. Y., & Kwok, S. 1991, A&A, 250, 179